Fırat Üniversitesi Müh. Bil. Dergisi
36(1), 437-445, 2024

Araştırma Makalesi
https://doi.org/10.35234/fumbd.1406375

Design, Fabrication and Performance Analysis of a Portable, Antenna Analyzer Based, Quartz Crystal Microbalance Measuring System with Energy Dissipation

Ceyhun Ekrem Kırımlı[1*]
[1] Department of Biomedical Engineering, Faculty of Engineering and Natural Sciences, Acıbadem Mehmet Ali Aydınlar University, Istanbul, Türkiye
ceyhun.kirimli@acibadem.edu.tr

(Geliş/Received: 18/12/2023; Kabul/Accepted: 19/03/2024)

Abstract: Impedance measurements play a critical role in analyzing the electrical behavior of piezoelectric biosensors in general. Antenna analyzers are engineered to measure the specific case of input impedance for antenna systems. In this study small form factor antenna analyzer is repurposed to work as driving circuit for a Quartz Crystal Microbalance (QCM) biosensor in combination with a single board computer as an indication of how small and portable an impedance measuring system can be made, while allowing monitoring of important parameters of series and parallel resonance frequencies together with dissipation factor. A QCM crystal with a 10 MHz fundamental resonance frequency is employed to determine the limit of detection of the system in Bovine Serum Albumin (BSA) and glycerol solutions. Dissipation factor and phase angle were monitored during the experiments. Limit of detection is 20 µg/ml BSA in phosphate buffer saline (PBS) and 250 µl of glycerol in 100 ml of deionized water.

Keywords: Quartz Crystal Microbalance, dissipation factor, phase angle, Bovine Serum Albumin, impedance measurement.

Enerji Yitimi Ölçebilen Taşınabilir Anten Analizörü Tabanlı Kuvars Kristal Mikroterazi Ölçüm Sisteminin Tasarımı, Üretimi ve Performans Analizi

Özet: Empedans ölçümü birçok piezoelektrik biyosensörün elektriksel davranışını analiz etmede kritik rol oynayan bir tekniktir. Anten analizörleri, anten sistemlerinin giriş empedansını ölçmek için tasarlanmıştır. Bu çalışmada bir empedans ölçüm sisteminin ne kadar küçük ve taşınabilir olabileceğinin bir kanıtı olarak, tek kartlı bir bilgisayarla kombinasyon halinde bir Kuvars Kristal Mikro Terazi (QCM) biyosensörü için sürüş devresi olarak çalışmak üzere küçük form faktörlü bir anten analizörü yeniden tasarlanmıştır. Seri ve paralel rezonans frekanslarının ve dağılım faktörünün önemli parametrelerinin izlenmesi 10 MHz temel rezonans frekansına sahip bir QCM kristali, sistemin Bovine Serum Albumin (BSA) ve Gliserol çözeltilerinde tespit limitini belirlemiştir. Deneyler sırasında dağılım faktörü ve faz açısı izlenmiştir. Saptama sınırı, fosfat tamponlu salinde (PBS) 20 µg/ml BSA ve 100 ml deiyonize suda 250 µl gliseroldür.

Anahtar kelimeler: Kuvars Kristal Mikroterazi, enerji yitim faktörü, faz açısı, sığır serum albümini, empedans ölçümü.

1. INTRODUCTION

QCM is a bulk acoustic wave piezoelectric biosensor where shear mode oscillations are used to determine natural frequency of the bulk material by means of resonance [1]. Shear mode oscillations require an AT cut of the quartz crystal, which has the highest thermally stable piezoelectric coefficients among all possible cuts [2]. QCM was first used in air or vacuum to measure weight deposited on the surface with sensitivity at microgram levels. Sauerbrey's equation [3] accurately converted a change in resonance frequency to the change in mass of the deposited material. QCM is still used in sputtering instruments and thermal deposition instruments to measure the thickness of deposited metal thin films at angstrom levels. Sauerbrey's equation however, cannot account for the large resonance frequency shift when the resonator is fully submerged in liquids. Kanazawa's work explained how the viscosity of the surround medium effects the resonance frequency as shown in Equation (1) [4]. With the help of further work of Voinova et. al. it was later demonstrated that, energy dissipation especially at the higher harmonics can be used to further understand not only viscosity of the medium but also the viscoelastic properties of the thin films deposited on the QCM surface in aqueous solutions [5].
There are different methods with which resonance frequency and/or dissipation factor can be determined electronically [6, 7]. Modern devices make use of the ring down method as it is the fastest way to measure these parameters. In the ring down method, QCM is first excited by applying an electrical potential at the resonance frequency with enough cycles to reach maximum oscillation amplitude. Then, the energy transfer is halted by turning of this driving voltage pattern, and the resonator is allowed to dissipate the loaded energy in time.

* Corresponding Author: ceyhun.kirimli@acibadem.edu.tr. Author's ORCID Number: [1] 0000-0001-7470-0059

Dissipation factor is determined as explained in Equation (2), from the voltage pattern generated by the piezoelectric crystal while the oscillations amplitudes fades in time [8].

Impedance measurements can also be used to determine dissipation factor by means of measuring amplitude of the impedance and conductance respectively [8]. Among all the different methods of driving QCM, impedance measurements, although are time consuming, generate the most information about the system[6, 7]. Almost all biosensor applications require high sensitivity where the concentration of the analyte is low and diffusion limits the reaction time for the analyte to bind on the QCM surface and reach equilibrium. Antenna and impedance analyzers can be used to measure impedance, where the former can be small in size and inexpensive in comparison. These devices are also used in the literature not only to drive QCM biosensors but also other piezoelectric biosensors [9-14]. Portability of these intruments is also another concern, especially for field applications. OpenQCM's NEXT is the only commercially available platform as of today that can measure resonance frequency and dissipation simultaneously, however it lacks the ability to take measurements in elevated temperatures and it does not come with a pump or PC or any other portable single board computer (SBC). There are also portable measurements systems in the literature[15-18]. Adel et. al.'s study uses a frequency counter and heating and cooling air conditioning (AC) system for the flow cell although the AC system is only demonstrated to work between 19^{o}C and 29 ^{o}C. which is not suitable for isothermal amplification techniques. Moreover the system does not include a portable pump and a PC is required and most importantly the system does not measure dissipation factor but only the resonance frequency [15]. Beißner et. al. developed an oscillator circuit with a control loop that can adjust the applied voltage driving the QCM. Although the chip design is interesting and robust, it only measures the resonance frequency shifts and no pumping system, PC or temperature control is integrated [16]. Liang et. al. developed a similar integrated circuit design and a flow cell lacking the ability to measure dissipation factor[17]. Muñoz et. al. developed a SBC based system with temperature control but only demonstrated a temperature range between 18^{o}C and 31^{o}C and the measurement device is a vector network analyzer which can simultaneously measure resonance frequency and dissipation factor. However, samples were injected using a syringe manually. In this study, a small form factor antenna analyzer circuit is combined to work in conjunction with a single board computer to fabricate a proof-of-concept QCM instrument capable of measuring both the resonance frequency and dissipation simultaneously. A peristaltic pump was designed, printed and integrated into the system to withstand temperatures above 95^{o}C, which would allow any isothermal amplification reaction. The developed system also has an integrated SBC and flow cell. In order to measure the performance of the system BSA and Glycerol solutions are used to find the limit of detection (LOD). As 10 MHz fundamental resonance frequency QCM resonators are used in the study and the maximum frequency that can be measured by the system is 30 MHz. only the fundamental resonance frequency and the third harmonic are utilized during the experiments which obstructed application of detailed viscoelastic models. LOD of glycerol and BSA were determined to be 250µl/100ml deionized water and 20 µg/ml in PBS buffer respectively.

2. MATERIALS AND METHODS

2.1 Portable Peristaltic Pump Design and Flow Cell

A portable peristaltic pump was designed in Autodesk Fusion 360 and 3D printed using a fused deposition modeling (FDM) type printer (Zonestar P802QR2). Acrylonitrile butadiene styrene (ABS) filament with a diameter of 1.75 mm was used as the sole 3d printed material. In the design 6 bearings (624zz) with inner diameter of 5mm, outer diameter of 13 mm and thickness of 4mm. Peristaltic pump tubing with an inner diameter 1.6mm and outer diameter of 3.2 mm (Tygon® formula 2375) was used to pump liquids at a flow rate of 100µl/min. Arduino Uno R3 controller board was used with a CNC shield, one A4988 driver. 16 microstepping is used with a NEMA13 step motor combined with a 51:1 planetary gearbox (14HS13-0804S-PG51). Grbl v1.1 was flashed into the Arduino to be used as the firmware and the gcode necessary to turn the stepper motor was sent through the serial port using python running on Raspberry Pi 4. The peristaltic pump system used in this study was a newer version of the one that is used by Cetin et.al.[19] The peristaltic pump and its components are shown in Figure 1.

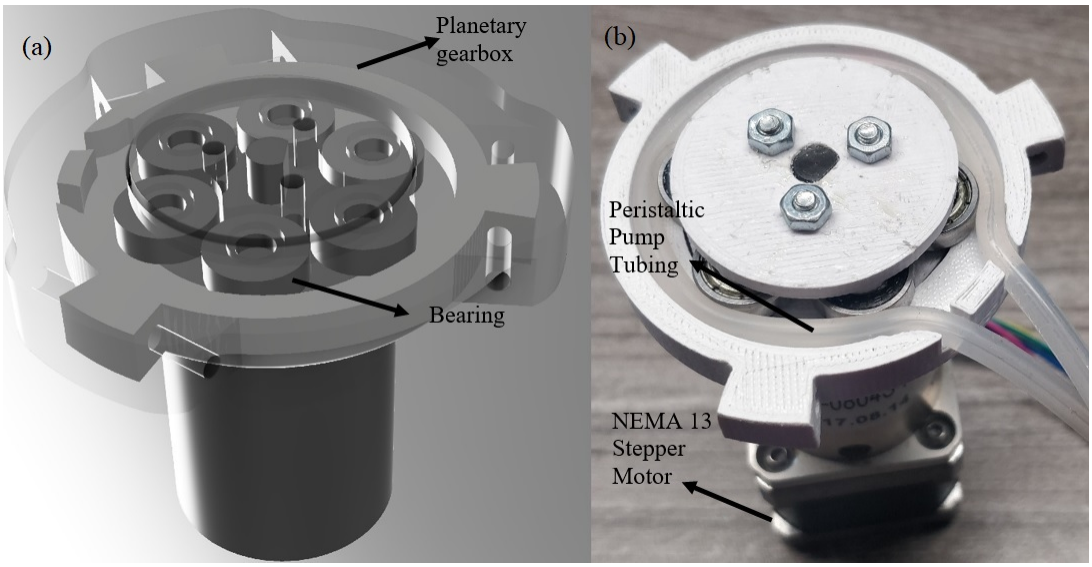

Figure 1. (a) 3D rendering of the peristaltic pump in Autodesk Fusion 360. Some parts are rendered transparent to illustrate the inner workings of the pump. (b) Peristaltic pump is printed and assembled (incompletely) to show the inner workings of the pump, as well as the tubing.

2.2 Connection of antenna analyzer with a Single Board Computer

An inexpensive vector high frequency antenna analyzer (Rigexpert AA-30.Zero) was chosen for this study. Important specifications of the antenna analyzer is summarized in Table 1. Maximum power consumption of the antenna analyzer is approximately 0.65 watts (5V DC voltage and max of 150 mA current). It weighs 65 gr and has a frequency range from 60kHz to 30 MHz with a frequency resolution of 1 Hz. It has a universal asynchronous receiver/transmitter (UART) communication interface with a 38400 baud rate. Raspberry Pi 4 Model B with 8 GB of ram is used as a single board computer. (Figure 2)

Table1. Specifications of the antenna analyzer used to monitor impedance of QCM.

Frequency range	0.06 to 30 MHz
Frequency resolution	1 Hz
Communication interface	UART, 38400 baud
SWR(standing wave ratio) measurement range	1 to 100

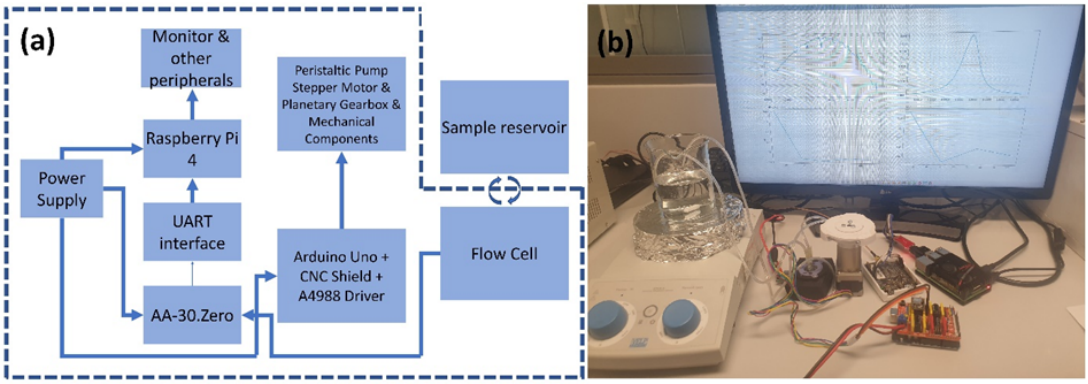

Figure 2. (a) A schematic diagram of the components of the systems. Arrows indicate how each component is connected to each other. Every component in the dashed line can be fitted in a portable enclosure. (b) A picture of the components during a detection experiment.

2.3 BSA and Glycerol LODExperiments

Glycerol (Sigma) and BSA (Sigma) are spiked in 100 ml deionized water and 100 ml 1x PBS buffer solutions respectively. Concentrations ranging from 250µl/100ml to 750 µl /100ml and from 20 µg/ml to 60 µg/100ml for Glycerol and BSA were prepared to measure LOD. Magnetic stirrer is used at room temperature to speed the diffusion and homogenize the solution before the solution reaches the flow cell for glycerol experiments. Flow cell had a total volume of 30 µl and the total volume of the liquid inside the tubing was approximately 1750 µl. For BSA detections 2ml Eppendorf tubes were used as sample reservoir and samples were vortexed for 30 seconds before experimentation. LOD experiments were performed as described before[20] in 3-sigma fashion. A standard deviation of the resonance frequency position was calculated by monitoring the phase angle peak position in time for 30 min in deionized water and 1x PBS for glycerol and BSA respectively. These values are determined to be 2.5 Hz at room temperature for deionized water and 3.5 Hz for 1xPBS solution. 200 data points were collected in each sweep at a fixed window size of 1 kHz for the fundamental resonance frequency around 10 MHz for the phase angle sweeps. Peak tracking was applied for phase angle sweeps. Each sweep's duration was approximately 25 seconds. For dissipation, 200 data points were collected at a fixed windows size of 4 kHz. Peak tracking was not applied for the conductance peak as the window was large enough to compensate for the low frequency shifts, especially at concentrations close to the LOD. Any shift bigger than 7.5 Hz for glycerol solutions ($\sigma_{glycerol}$=2.5Hz) and 10.5 Hz for BSA in 1x PBS solutions (σ_{1xPBS}=3.5 Hz) were considered as detection and LOD were measured as the lowest such concentrations for each analyte.

2.4 Data Collection and Analysis

Miniconda is installed in the Raspberry Pi 64 bit operating system. Spyder compiler is used to write a routine to control not only the peristaltic pump, but also the parameters of AA-30.Zero during impedance measurements as explained before[9, 20]. Resonance frequency and dissipation factor was calculated and plotted in real time as can be seen in Figure 3. Real time monitoring of the resonance frequency shift was achieved by measuring the phase angle of the impedance, and sweep window was adjusted to track the moving peak position in time as discussed before[9, 20]. Dissipation factor, D, was calculated from the conductance peak as described before using the equation (1) [8].

For this, a baseline is first measured from the average of the first 3 and last 3 values of the conductance measurement, as shown in Figure 3 below. The frequency of the peak point of the conductance was used to determine the height of the conductance peak, which is then used to calculate the half-maximum of the peak. The width at this level is then calculated from the 4 discrete data points of the conductance graph that are closest in distance. These 4 points were then used to calculate the equation of the lines passing through them as shown in figure 3. The distance between intersections of these lines with the half-maximum is used to calculate the Full Width at Half Maximum (FWHM). This value is then divided by the frequency of the peak position to calculate the dimensionless dissipation factor finally as in (1).

$$D = \frac{FWHM}{f_0} \tag{1}$$

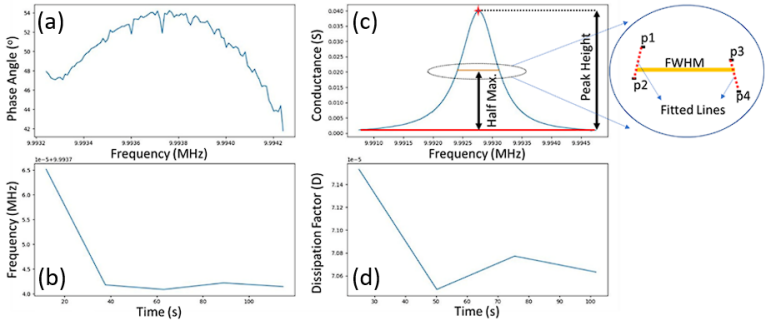

Figure 3. (a) Frequency (Hz) vs phase angle(degrees) data measured in the last sweep. (b) Time (seconds) vs peak position of the phase angle (Hz) plot showing time evolution of the peak position during detection. (c) Frequency vs Conductance (siemens,S) data measured in the last sweep. Inset to the right is a schematic illustrating how the FWHM is determined from the half maximum line. (d) Time(seconds,s) vs Dissipation factor (D,dimensionless) plot showing time evolution of the dissipation factor during detection.

3. FINDINGS AND DISCUSSION

Figure 4a shows the results of the limit of detection experiments for glycerol detections. 3 different concentrations, 250 µl, 500 µl and 750 µl of glycerol dissolved in 100 ml of deionized water, are detected 3 times each. LOD was measured to be 250 µl of glycerol in 100ml of deionized water. This was, in comparison to best performing portable antenna analyzer (RigExpert Stick 230) from the same manufacturer, less than 1.5 times less sensitive. Shaded area in figure 4a represents the standard deviation of all 3 detections in each concentration. A frequency shift of ≈8.5 Hz was measured at LOD. Equation (2) was used to calculate the viscosity of the glycerol mixtures from the frequency shifts.

$$\Delta f = -f_0^{3/2} \cdot \left(\frac{\eta_L \rho_L}{\pi \mu_Q \rho_Q}\right)^{1/2} \quad (2)$$

In Equation (2), Δf represents resonance frequency shift. This is calculated from the average resonance frequency position between 27th-30th min. following the spiking of the glycerol into the deionized water. η_L and ρ_L represent the absolute viscosity of the liquid (0.01002 g/(cm.s) at room temperature) and density of the liquid (0.9982 g/cm^3 at room temperature) respectively. μ_Q and ρ_Q represents the shear modulus of the quartz crystal (2.947 x 10^{11} g/(cm.s^2)) and density of the quartz (2.648 g/cm^3) respectively.These viscosity values are then used to calculate the resonance frequency shifts (Δf) and the measured and known concentrations are plotted in figure 4b using tables as described before [20]. ΔD vs time graphs were also plotted in Figure 4c. As expected, the frequency shift and dissipation factor shifts were inversely proportional as energy dissipation increased as the viscosity of the bulk fluid increased with the increasing concentrations of Glycerol. Unfortunately viscoelastic properties of the bulk liquid cannot be determined as dissipation factor and resonance frequency shifts of higher harmonics are required for such models [5] and fundamental resonance peak is usually omitted.

When compared to the previous results with different antenna analyzers from the same manufacturer, AA-30.Zero gave the least performance in terms of LOD. This was expected as, in comparison to those, it is slower and hence less accurate. Sweep rate is important in the sense that less data points can be collected at a given time lowering the time resolution of each sweep, making it more difficult to determine the peak position from a sweep using the algorithm described before [9].

To measure the performance of the system using an analyte not only increasing the viscosity of the bulk fluid as glycerol, BSA was used as it can be physically adsorbed even on a gold electrode. BSA concentration were prepared in 1x PBS buffer as in most biosensor studies involving detection of analytes based on proteins or small peptides, BSA is used as a remedy to overcome the non-specific binding problem [21-24]. Δf and ΔD vs time shifts of concentrations ranging from 20 µg/ml to 60 µg/ml were plotted in Figure 5a and 5b respectively. LOD of BSA in 1xPBS solutions were determined to be 20 µg/ml. Frequency shifts in each concentration after 30min are also plotted in figure 5c.

3.1 Conclusion and Evaluations

A portable impedance based QCM biosensing system was designed and prototyped as proof of concept in this study. All the components are 3d printed and a single board computer was utilized to analyze data in real time. To measure the performance of the system, BSA and glycerol solutions were prepared and LODs were measured. AA30.zero antenna has a very small form factor; however, the analysis of real time data requires computing power which requires the use of single board computer. Majority of power consumed by the system is not due the measurements but mainly due to the Raspberry Pi 4 computer and peristaltic pump. To reduce the power consumption of the peristaltic pump, NEMA13 stepper motor was used instead of NEMA17. The motor draws 0.6 A at 20V. Total system power was ≈18 watts including the Raspberry Pi 4, which is very high as it would take ≈4 hrs to deplete a commercially available 20000 mAh power bank. This could be improved by using a more efficient SBC or a smaller stepper motor as torque was already increased using a 51:1 planetary gearbox.

The system can be developed as two parts in the future, consisting of a driving system including the SBC and the antenna analyzer and a second component consisting of the flow cell and the peristaltic pump. Temperature resistant stepper motors are available that can withstand ambient air temperatures up to 130 oC. When combined with temperature resistant small inner diameter peristaltic pump tubing this second component could be fitted inside a drying oven so that biosensing can be achieved at elevated temperatures with an exceedingly small (<100µl) sample volume for the fraction of the price of an equivalent QCM device. Machine learning algorithms can also be run on impedance measurements of QCM biosensors as studied before [20] and modern SBCs are

already equipped with central processing units (CPUs) and random access memory (RAM) enough to cope with such light machine learning loads. Further work in this direction has already been initiated by the researcher.

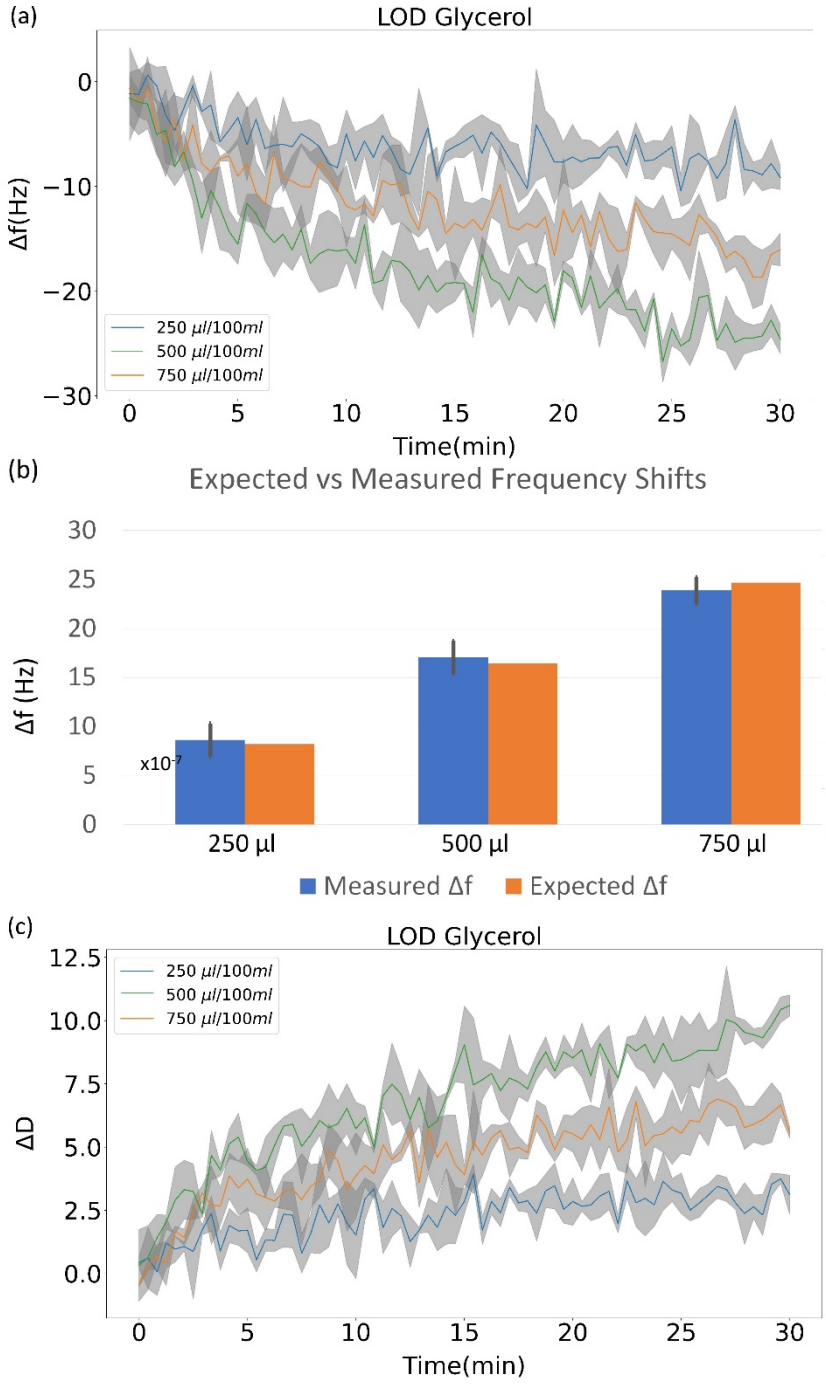

Figure 4. (a) Resonance frequency shifts of observed when 250 µl, 500 µl and 750 µl of liquid is dissolved in deionized water. (b) Expected and measured resonance frequency shifts due to viscosity change of the bulk liquid. (c) Dissipation factor shift due to viscosity change of the bulk liquid. Shaded area represents the standard error in 3 experiments for each concentration.

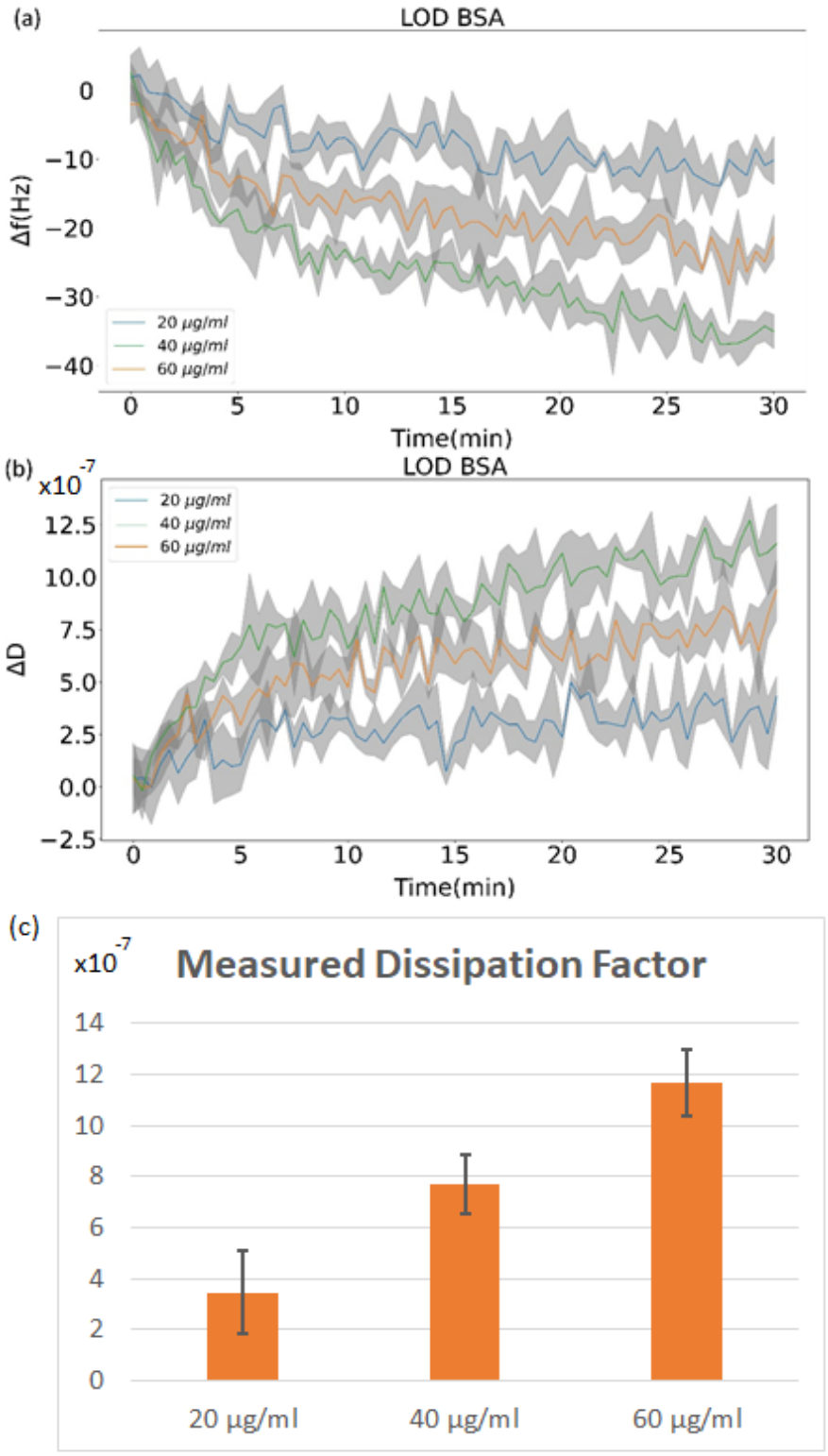

Figure 5. (a)Resonance frequency shifts of observed when 20 µg/ml, 40 µlml and 60 µg/ml of BSA is dissolved in 1x PBS. (b) Dissipation factor shift due to adsorption of BSA on QCM surface for the same concentrations. Shaded area represents the standard error in 3 experiments for each concentration. (c) Represents the average dissipation factor change in the last 3 minutes (28^{th} till 30^{th} min) of each experiment.

References

[1] Johannsmann D. *The Quartz Crystal Microbalance in Soft Matter Research : Fundamentals and Modeling*, 1st ed. Cham: Springer International Publishing : Imprint: Springer,, 2015, pp. 1 online resource (XX, 387 pages 123 illustrations, 9 illustrations in color.

[2] Soewito B. "Designing and Manufacturing Quartz Crystal Oscillators," in *Computational Intelligence and Efficiency in Engineering Systems*, G. Borowik, Z. Chaczko, W. Jacak, and T. Łuba Eds. Cham: Springer International Publishing, 2015, pp. 293-306.

[3] Sauerbrey G. "Verwendung von Schwingquarzen zur Wägung dünner Schichten und zur Mikrowägung," *Zeitschrift für Physik,* vol. 155, no. 2, pp. 206-222, 1959/04/01 1959, doi: 10.1007/BF01337937.

[4] Keiji Kanazawa K, Gordon JG. "The oscillation frequency of a quartz resonator in contact with liquid," *Anal Chim Acta,* vol. 175, pp. 99-105, 1985/01/01/ 1985, doi: https://doi.org/10.1016/S0003-2670(00)82721-X.

[5] Voinova MV, Rodahl M, Jonson M, Kasemo B. "Viscoelastic Acoustic Response of Layered Polymer Films at Fluid-Solid Interfaces: Continuum Mechanics Approach," *Phys. Scr.,* vol. 59, no. 5, p. 391, 1999/05/01 1999, doi: 10.1238/Physica.Regular.059a00391.

[6] Alassi A, Benammar M, Brett D. "Quartz Crystal Microbalance Electronic Interfacing Systems: A Review," *Sensors-Basel,* vol. 17, no. 12, p. 2799, 2017. [Online]. Available: https://www.mdpi.com/1424-8220/17/12/2799.

[7] Arnau A. "A Review of Interface Electronic Systems for AT-cut Quartz Crystal Microbalance Applications in Liquids," *Sensors-Basel,* vol. 8, no. 1, pp. 370-411, 2008. [Online]. Available: https://www.mdpi.com/1424-8220/8/1/370.

[8] Banica F-G. *Chemical sensors and biosensors : fundamentals and applications*. Chichester, West Sussex, United Kingdom: Wiley, 2012, pp. xxxiii, 541 pages.

[9] Kirimli CE, Shih W-H, Shih WY. "DNA hybridization detection with 100 zM sensitivity using piezoelectric plate sensors with an improved noise-reduction algorithm," *Analyst,* vol. 139, no. 11, pp. 2754-2763, 2014.

[10] Kirimli CE, Shih W-H, Shih WY. "Specific in situ hepatitis B viral double mutation (HBVDM) detection in urine with 60 copies ml− 1 analytical sensitivity in a background of 250-fold wild type without DNA isolation and amplification," *Analyst,* vol. 140, no. 5, pp. 1590-1598, 2015.

[11] Kirimli CE, Shih W-H, Shih WY. "Amplification-free in situ KRAS point mutation detection at 60 copies per mL in urine in a background of 1000-fold wild type," *Analyst,* vol. 141, no. 4, pp. 1421-1433, 2016.

[12] Kirimli CE, Shih W-H, Shih WY. "Piezoelectric Plate Sensor (PEPS) for Analysis of Specific KRAS Point Mutations at Low Copy Number in Urine Without DNA Isolation or Amplification," *Biosensors and Biodetection: Methods and Protocols, Volume 2: Electrochemical, Bioelectronic, Piezoelectric, Cellular and Molecular Biosensors,* pp. 327-348, 2017.

[13] Kirimli CE, Elgun E. "A Comparison of Impedance and Antenna Analyzers on the Basis of Machine Learning Assisted Limit of Detection Experiments," in *2022 International Workshop on Impedance Spectroscopy (IWIS)*, 27-30 Sept. 2022 2022, pp. 61-65, doi: 10.1109/IWIS57888.2022.9975132.

[14] Muckley ES, Collins L, Srijanto BR, Ivanov IN. "Machine Learning-Enabled Correlation and Modeling of Multimodal Response of Thin Film to Environment on Macro and Nanoscale Using "Lab-on-a-Crystal"," *Adv. Funct. Mater.,* https://doi.org/10.1002/adfm.201908010 vol. 30, no. 10, p. 1908010, 2020/03/01 2020, doi: https://doi.org/10.1002/adfm.201908010.

[15] Adel M, Allam A, Sayour AE, Ragai HF, Umezu S, Fath El-Bab AMR. "Design and development of a portable low-cost QCM-based system for liquid biosensing," *Biomed. Microdevices,* vol. 26, no. 1, p. 11, 2024/01/18 2024, doi: 10.1007/s10544-024-00696-0.

[16] Beißner S *et al.*, "Low-cost, in-liquid measuring system using a novel compact oscillation circuit and quartz-crystal microbalances (QCMs) as a versatile biosensor platform," *J. Sens. Sens. Syst.,* vol. 6, no. 2, pp. 341-350, 2017, doi: 10.5194/jsss-6-341-2017.

[17] Liang J, Zhang J, Wang P, Liu C, Qiu S, Ueda T. "Development of Portable Quartz Crystal Microbalance for Biosensor Applications," *Sens. Mater.,* vol. 28, no. 3, 2016.

[18] Muñoz GG *et al.*, "Quartz crystal Microbalance with dissipation monitoring for biomedical applications: Open source and low cost prototype with active temperature control," *HardwareX,* vol. 14, p. e00416, 2023/06/01/ 2023, doi: https://doi.org/10.1016/j.ohx.2023.e00416.

[19] Cetin I, Yilmaz G, Halilibrahimoglu H, Kirimli CE. ""Do It Yourself" Peristaltic Pump and Flowcell for QCM Biosensor," in *2017 21st National Biomedical Engineering Meeting (BIYOMUT)*, 24 Nov.-26 Dec. 2017 2017, pp. i-iv, doi: 10.1109/BIYOMUT.2017.8479100.

[20] Kirimli CE, Elgun E, Unal U. "Machine learning approach to optimization of parameters for impedance measurements of Quartz Crystal Microbalance to improve limit of detection," *Biosens. and Bioelectron.: X,* vol. 10, p. 100121, 2022/05/01/ 2022.

[21] Andersson L-O, Rehnström A, Eaker DL. "Studies on "Nonspecific" Binding," *Eur. J. Biochem.,* https://doi.org/10.1111/j.1432-1033.1971.tb01403.x vol. 20, no. 3, pp. 371-380, 1971/06/01 1971.

[22] Reimhult K, Petersson K, Krozer A. "QCM-D Analysis of the Performance of Blocking Agents on Gold and Polystyrene Surfaces," *Langmuir,* vol. 24, no. 16, pp. 8695-8700, 2008/08/01 2008, doi: 10.1021/la800224s.

[23] Xiao Y, Isaacs SN. "Enzyme-linked immunosorbent assay (ELISA) and blocking with bovine serum albumin (BSA)—not all BSAs are alike," *J. Immunol. Methods,* vol. 384, no. 1, pp. 148-151, 2012/10/31/ 2012, doi: https://doi.org/10.1016/j.jim.2012.06.009.

[24] Dolatshahi-Pirouz A, Rechendorff K, Hovgaard MB, Foss M, Chevallier J, Besenbacher F. "Bovine serum albumin adsorption on nano-rough platinum surfaces studied by QCM-D," *Colloids Surf. B,* vol. 66, no. 1, pp. 53-59, 2008/10/01/ 2008, doi: https://doi.org/10.1016/j.colsurfb.2008.05.010.